Microchimica Acta (2019) 186: 738
https://doi.org/10.1007/s00604-019-3826-6

ORIGINAL PAPER

Hollow Prussian Blue nanocubes as peroxidase mimetic and enzyme carriers for colorimetric determination of ethanol

Shuangling Wang[1] · Han Yan[1] · Yalin Wang[1] · Na Wang[1] · Yulong Lin[1] · Meng Li[1]

Received: 4 May 2019 / Accepted: 14 September 2019 / Published online: 1 November 2019

Abstract

The peroxidase-like activity of hollow Prussian Blue nanocubes (hPBNCs) is used, in combination with the enzyme alcohol oxidase (AOx), in a colorimetric ethanol assay. Different from other nanozymes, the large cavity structure of the hPBNCs provides a larger surface and more binding sites for AOx to be bound on their surface or in the pores. This extremely enhances the sensitivity of the assay system. In the presence of ethanol, AOx is capable of catalyzing the oxidation of alcohols to aldehydes, accompanied by the generation of hydrogen peroxide (H_2O_2). The hPBNCs act as peroxidase mimics and then can catalyze the oxidation of 3,3′5,5′-tetramethylbenzidine (TMB) by H_2O_2, resulting in a color change of the solution from colorless to blue with a strong absorption at 652 nm. The lower detection limit for ethanol is 1.41 μg·mL^{-1}. Due to the high catalytic activity of hPBNCs in weakly acidic and neutral solutions, the system was successfully applied to the determination of ethanol in mice blood. This is critically important for studying the alcohol consumption and monitoring the ethanol toxicokinetics.

Keywords Nanozymes · Nanocomposites · Cavity structure · Catalytic activity · Alcohol oxidase · Hydrogen peroxide · Chromogenic substrate · Blood analysis · Ethanol toxicokinetics · Optical sensor

Introduction

Alcohol over-consumption has been reported to lead to variety of diseases, disorders and many types of injury, which would result in approximately 2.5 million deaths each year [1–3]. Owing to the significance of its toxicokinetics, the accurate and sensitive determination of alcohol level in vivo is of particular interest, especially its concentration dynamics. To measure alcohol consumption, different methods for detection of the concentration of alcohol in blood, urine, breath, sweat, saliva or other body fluids have been demonstrated [4–7], in which blood alcohol concentration is recognized as the most widely used indicator of alcohol intoxication. Thus, sensitive detection and quantification of alcohol in blood has important significance for diagnostic and therapeutic implications. For this purpose, a series of methods and techniques for accurate and precise determination of alcohol level in blood have been employed, including gas chromatography [8], liquid chromatography [9], spectroscopy [10–14], and electrochemical analysis [15, 16].

Among these methods, ethanol conversion enzymes based biosensors for detection of alcohol concentration in blood are widely developed due to their simplicity, low cost, rapidity, high sensitivity and selectivity [17]. With this motivation, ethanol-sensitive biosensors [18] were constructed using alcohol oxidase (AOx) or alcohol dehydrogenase (ADH) as the bio-recognition components of the biosensors. Compared with the commonly used ADH, AOx can irreversibly oxidize primary alcohol and contains the flavin-based co-factor which is avidly associated with the redox center of the enzyme, making it more pertinent for biosensor design [18, 19]. In this way, hydrogen peroxide (H_2O_2) generated in situ from the AOx catalysed oxidation of alcohol in the presence of oxygen. With the development of H_2O_2 sensors, various electrochemical methods as well as fluorescent or colorimetic approaches based on synthetic probes and enzymes have been developed

Electronic supplementary material The online version of this article (https://doi.org/10.1007/s00604-019-3826-6) contains supplementary material, which is available to authorized users.

✉ Yulong Lin
linyulong8@163.com

✉ Meng Li
limeng87@hotmail.com

[1] School of Pharmaceutical Sciences, Hebei Medical University, Zhongshan East Road 361, Shijiazhuang 050017, People's Republic of China

to monitor the alcohol concentration in blood via the detection of the produced H_2O_2 [18, 20–22].

Nanomaterials as peroxidase mimics used to detect H_2O_2 have received abundant attention [23] since the first peroxidase-like activity of Fe_3O_4 nanoparticles was reported [24]. Various nanomaterials, including carbon-based nanomaterials [25], metal organic frameworks [26] as well as metallic nanocomposites [27] have been demonstrated to exhibit peroxidase-like activity. Prussian Blue based nanomaterials (PBNMs), as a prototype for transition metal hexacyanoferrates, have also been shown to possess the intrinsic peroxidase-like activity and been employed as the electron-transfer mediators in electrochemical sensors for H_2O_2 detection [28]. Although PBNMs provide a high stability and an excellent peroxidase-like activity, colorimetric approaches based on PBNMs are still rare [29, 30].

Herein, utilizing the peroxidase-like activity of hollow Prussian Blue nanocubes (hPBNCs) [30] and AOx, a novel colorimetric assay for sensitively and accurately monitoring ethanol concentration in blood is developed (Fig. 1). In the presence of alcohols, AOx is capable of catalyzing the oxidation of alcohols to aldehydes, accompanied by the generation of H_2O_2. With the peroxidase-like activity, hPBNCs then can catalyze the oxidation of 3,3′5,5′-tetramethylbenzidine (TMB) by the produced H_2O_2, resulting in a color change of the solution from colorless to blue. Critically, different from other

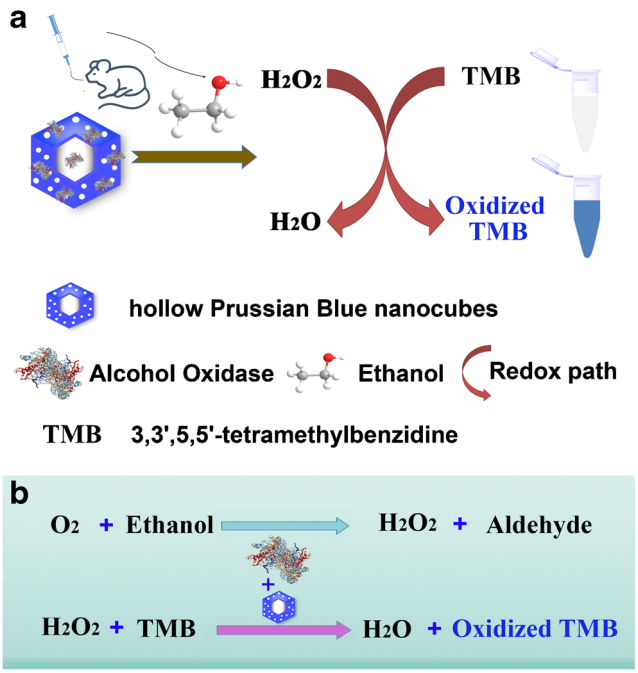

Fig. 1 **a** Schematic illustration of colorimetric assay for tracking ethanol concentrations by using peroxidase-like activity of hPBNCs and the ethanol conversion enzyme, AOx. **b** The principle of the assay for ethanol detection. In the presence of ethanol, AOx is capable of catalyzing the oxidation of ethanol to aldehyde, accompanied by the generation of H_2O_2. hPBNCs then can oxidize TMB to the oxidized TMB by the produced H_2O_2 to induce a color change of the solution from colorless to blue>

PBNMs, the large cavity structure of the hPBNCs provides a higher surface area and more binding sites for AOx to be bound on the surface of hPBNCs or encapsulated in the pores of hPBNCs. This makes hPBNCs as suitable carriers for AOx. With the sensitivity of AOx to alcohols and high catalytic activity of hPBNCs in physiological conditions, our assay can differentiate well between alcohols and other biomolecules. And the assay is appropriate for continuous ethanol monitoring in blood. To the best of our knowledge, this is the first report that hPBNC is used as both enzyme carrier and peroxidase-mimic for colorimetric sensing of ethanol.

Experimental

Chemicals and materials

Polyvinylpyrrolidone (PVP, MW 58000) and ascorbic acid (99%) were bought from J&K Chemical Ltd. (http://www.jkchemical.com). Potassium ferricyanide ($K_3[Fe(CN_6)]$, ≥99.5%) was supplied by Tianjin Bodi Chemical Co., Ltd. (Tianjin, China, http://bdhg.company.lookchem.cn). Hydrochloric acid (HCl, 36%–38%), ethanol (≥99.7%), Isopropyl alcohol (≥99.7%), butanol (≥99.5%) and methanol (≥99.5%) were obtained from Sinopharm Chemical Reagent Co., Ltd. (China, http://www.reagent.com.cn). Alcohol oxidase from Pichia pastoris (AOx, 26 $U \cdot mg^{-1}$ protein) and glucose (≥99.5%) were bought from Sigma-Aldrich (St. Louis, MO, USA, https://www.sigmaaldrich.com). 3,3′,5,5′-tetramethylbenzidine (TMB, >98%) and α-lactose monohydrate (>99%) were supplied by Adamas-beta (Shanghai, China, http://www.adamas-beta.com). Dopamine hydrochloride and Peroxidase from horseradish (HRP, >200 $U \cdot mg^{-1}$) were purchased from Aladdin Ltd. (Shanghai, China, http://www.aladdin-e.com). Hydrogen peroxide (H_2O_2, ≥30%) was obtained from Beijing Chemicals (Beijing, China, http://www.crc-bj.com). All the reagents in our study were not further purified and used as received.

Instruments

Powder X-ray diffraction (XRD) patterns were recorded with a Bruker AXS D8 Advance diffractometer (Cu-Kα radiation, λ = 1.5406 Å) (Germany, https://www.bruker.com/). The TU-1950 (Beijing Purkinje General Instrument Co., Ltd., http://www.pgeneral.com/) spectrophotometer was employed to monitor the UV-Vis absorption spectra. Transmission electron microscopy (TEM) images were taken using a Hitachi H-7650B microscope operating at 200 kV (Japan, https://www.hitachi-hightech.com/global/). Fourier transform infrared spectroscopy (FTIR) analysis was performed on a BRUKER Vertex 70 FTIR sp7ectrometer (Germany, https://www.bruker.com/).

Synthesis of hollow Prussian blue nanocubes (hPBNCs)

Firstly, 132 mg of $K_3[Fe(CN)_6]$ and 3.0 g of PVP were added to the HCl solution (0.01 M, 40 mL) under stirring. After the solution became clear, the solution was heated at 80 °C for 24 h in a stainless autoclave. The precipitates (the mesoporous Prussian Blue nanoparticles, MPBs) were collected by centrifugation (12,000 rpm, 8 min) and washed twice with distilled water. Then, the MPBs solution (1 mg·mL^{-1}) was mixed with 5 mg·mL^{-1} of PVP under magnetic stirring. Following stirring for 3 h, the mixture was put into the stainless autoclave and heated at 140 °C for 4 h. After centrifugation (12,000 rpm, 8 min), the precipitates were washed repeatedly with distilled water.

Characterization of interaction of hPBNCs with AOx

A 500 μL amount of AOx solution (1.2 mg·mL^{-1}, 31.2 U·mL^{-1}) was mixed with 125 μg of hPBNCs, and then incubated for 60 min at 37 °C. After that, the mixture was centrifuged and washed by the phosphate buffered saline (PBS) buffer. The supernatant was all collected and used for UV/vis absorbance detection. The AOx bound efficiency was calculated from the different absorbance intensities at 276 nm between the original AOx solution and the supernatant, which was determined to be 3.0 mg·mg^{-1} hPBNCs (77.7 U·mg^{-1} hPBNCs).

Determination of ethanol

For the detection of ethanol, 4 μL TMB (42 mM), 4 μL hPBNCs-AOx (the concentration of hPBNCs was 500 μg·mL^{-1}), and 4 μL different concentrations of ethanol were successively added into 388 μL PBS buffer (pH 7.0). The mixture solution was allowed to be incubated at room temperature for 20 min to enable complete oxidation of alcohols by AOx, followed by the spectral measurements. To detect the ethanol in the presence of serum, the mice serum was diluted 1:125 in PBS (pH 7.0) and used in one day after collection. Then the same experiments were carried out using the diluted serum instead of PBS.

Animal experiment

Adult male C57BL6/J mice, weighing between 20 g and 25 g, were purchased from the Experimental Animal Center of the Chinese Academy of Medical Sciences. The animal handing procedures were carried out accordance with the guidelines of the Hebei committee for care and use of laboratory animals, and were approved by the Animal Experimentation Ethics Committee of the Hebei Medical University. The mice were raised in a germ-free environment with free access to food and water. The mice, 6 per group, were treated intragastrically with different concentrations of ethanol (2 μL·g^{-1} B.W., 4 μL·g^{-1} B.W., 8 μL·g^{-1} B.W., 16 μL·g^{-1} B.W.). Blood was collected at different time points after intragastric administration and centrifuged to obtain plasma for the detection of ethanol concentration. When detected, the mice serum was diluted 1:125 in PBS (pH 7.0).

Results and discussion

Synthesis and characterization of the hPBNCs and hPBNCs-AOx

To demonstrate the feasibility of our approach, hPBNC was first synthesized via a hydrothermal method on the basis of MPB, followed by a PVP protected hydrochloric acid-etching process [30, 31]. As exhibited in the XRD patterns (Fig. 2a), hPBNCs reveals the well-defined PB crystal structure (JCPDS no. 73–0687) [31]. In addition, no other peaks can be detected, indicating that no other phases occur during the hydrothermal reaction process. FTIR spectroscopy is also employed to further characterize the chemical composition of hPBNCs. The peak at 2082 cm^{-1} is assigned to the -CN- stretching in the Fe-CN-Fe bond of hPBNCs, and the C=O stretching in the PVP amide unit appears at 1650 cm^{-1} (Fig. 2b) [31]. The monodisperse hPBNCs are cube in morphology with an average particle diameter of 80 nm, which is demonstrated by TEM image (Fig. 2c). In addition, sufficiently large numbers of particles (at least 200) are counted in TEM measurement to give access to the information on representative size distribution and morphology. Furthermore, a characteristic PB peak at approximately 708 nm is observed in the UV-vis-NIR absorbance spectrum of hPBNCs, which is consistent with the previous reports [30, 31] (Fig. S1). To show whether AOx can be adsorbed by hPBNCs, we incubated AOx with hPBNCs in advance. As shown in Fig. S2, AOx can associate with hPBNCs with an efficiency of 3.0 mg·mg^{-1} hPBNCs (77.7 U·mg^{-1} hPBNCs) which is calculated from the difference of the absorbance intensity at 276 nm between the AOx solution before and after incubation with hPBNCs. TEM images indicate that after binding or loading with AOx, no clear difference in shape and average diameter of the hPBNCs, but a protein corona is formed on the surface of hPBNCs, which suggests that AOx can not disturb the structure of hPBNCs (Fig. 2d). To verify the stability of hPBNCs-AOx, we maintained hPBNCs-AOx in buffered solutions for at least 7 days. As shown in Fig. S2 and Fig. S3, the supernatant of hPBNCs-AOx solution exhibits no absorbance at 276 nm and hPBNCs-AOx retain their

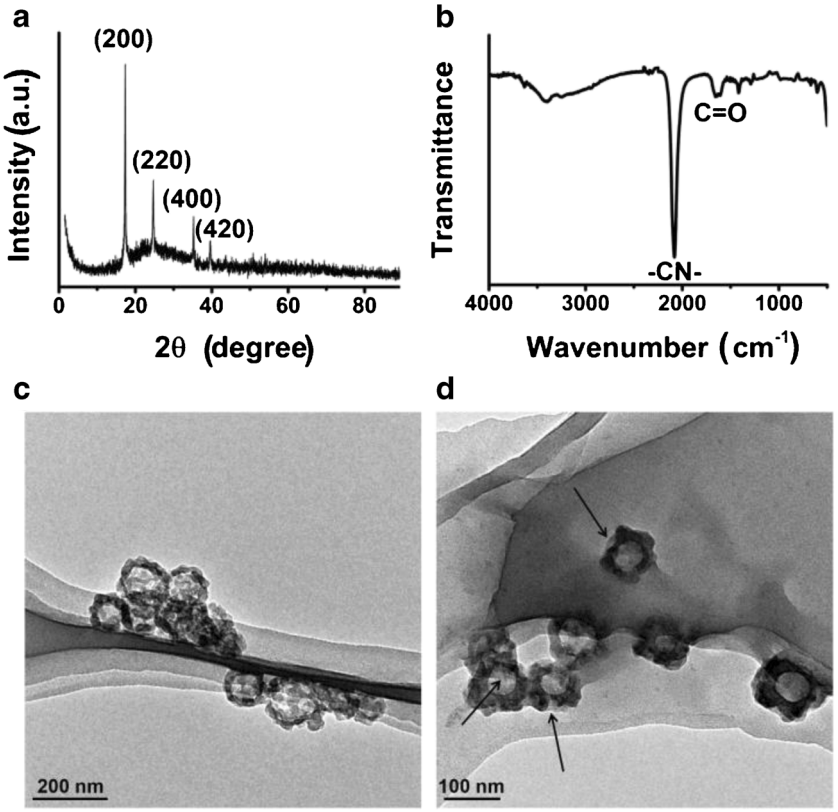

Fig. 2 The characterization of hPBNCs and hPBNCs-AOx. **a** The Wide-angle powder XRD pattern of hPBNCs. **b** FTIR spectra of hPBNCs. **c** TEM image of hPBNCs. **d** TEM image of hPBNCs-AOx. TEM image showed that a AOx corona (arrows) was formed on the surface of hPBNCs

protein corona structure, indicating the high stability of hPBNCs-AOx in buffered solutions.

The peroxidase-like activity of hPBNCs-AOx

Having demonstrated the successful synthesis of hPBNCs-AOx, the peroxidase-like activity of this novel nanocomposites that is directly impacted on the feasibility of the biosensor is subsequently investigated. The catalytic ability of hPBNCs toward TMB, the most commonly used peroxidase substrate, is firstly evaluated. As shown in Fig. 3, after incubation of hPBNCs with TMB in the presence of H_2O_2 for 10 min at room temperature, the solution exhibits an obvious blue color change, with a strong absorption at 652 nm. Furthermore, the catalytic activity of hPBNCs is increased in a concentration-dependent manner (Fig. S4). All these results indicate that the hPBNCs possess an intrinsic peroxidase-like activity which is quite similar to horseradish peroxidase (HRP) [30, 32]. The hPBNCs with the hollow structure can also increase the diffusion of small active molecules in and out of the nanomaterials, leading to the enhanced catalytic activity of hPBNCs. Furthermore, the vibration of free electrons between Fe^{2+} and Fe^{3+} and the superior stability in physiological conditions endow the hPBNCs with high peroxidase-like activity in vivo. The optimal concentration of hPBNCs is chosen as 5 $\mu g \cdot mL^{-1}$ for our subsequent experiment. Importantly, after binding with AOx, the catalytic activity of hPBNCs exhibits almost unchanged (Fig. 3). In contract, neither AOx nor H_2O_2 with TMB system can induce any color change (Fig. 3), indicating that addition of AOx into the system can not

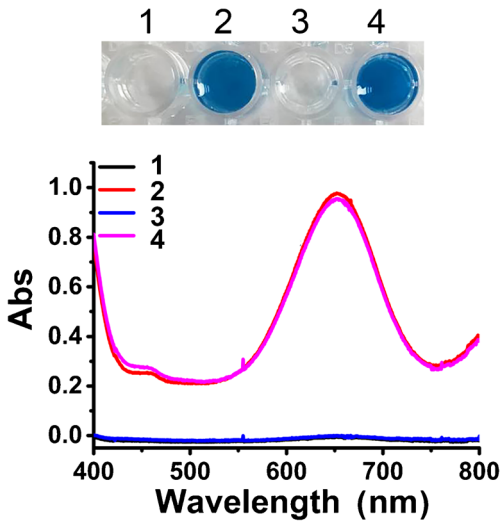

Fig. 3 The peroxidase mimetic properties of hPBNCs and hPBNCs-AOx. The absorbance spectra of TMB in different reaction systems: (1) H_2O_2 + TMB, (2) hPBNCs + TMB + H_2O_2, (3) AOx + TMB + H_2O_2, (4) hPBNCs-AOx + TMB + H_2O_2 in PBS (pH 7.0) at room temperature after 10 min incubation. Above were the visual color changes of TMB in the corresponding solutions

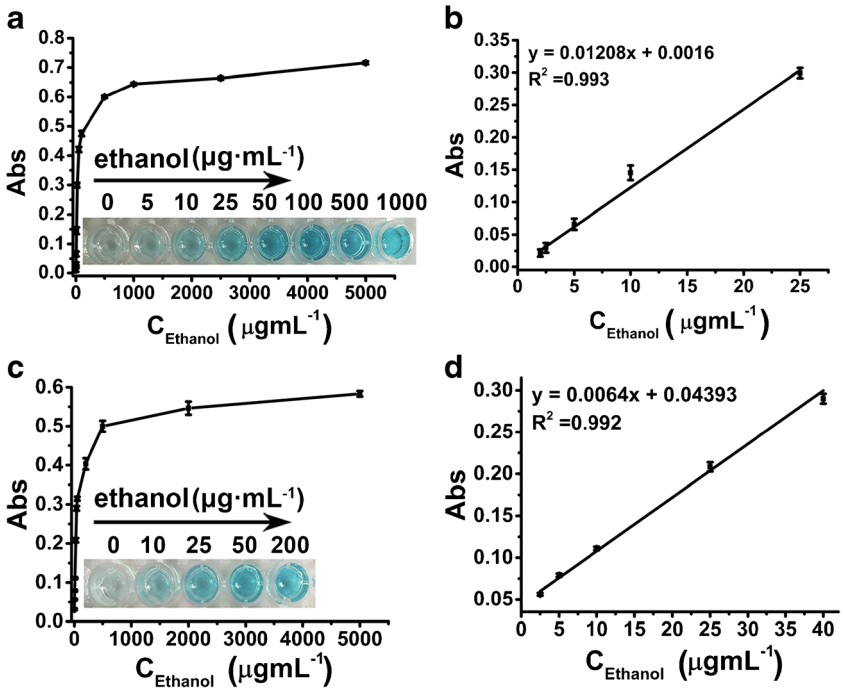

Fig. 4 Determination of ethanol by hPBNCs-AOx. **a** A dose-response curve for ethanol detection at 652 nm under the optimum conditions. **b** The linear plots of absorbance measured at 652 nm as a function of the ethanol concentration. **c** Detection of ethanol in the presence of serum. **d** The linear plots of absorbance measured at 652 nm as a function of the ethanol concentration in serum. Inset were the visual color changes of TMB in the corresponding solutions. (Mean ± SD, $n = 3$ for each sample)

affect the catalytic ability of hPBNCs. On the other hand, the influence of hPBNCs on the activity of AOx to catalyze the oxidation of ethanol is also investigated. As illustrated in Fig. S5, there is no obvious difference between the catalytic activity of AOx and hPBNCs-AOx. All these results demonstrate that hPBNCs-AOx can be used as an effective probe for colorimetric sensing of alcohol. Like other nanomaterial-based peroxidase mimics, the hPBNCs exhibit a temperature and pH value-dependent catalytic activity. The activities of both hPBNCs and hPBNC-AOx decrease with the increase of temperature (Fig. S6). Considering the practical operability and the sensitivity of this assay, room temperature is chosen as the optimal temperature for our subsequent experiment. Most notably, a relatively high catalytic activity for both hPBNCs and hPBNCs-AOx is observed over a broad range of pH values, especially in weakly acidic and neutral solutions, making them suitable for applications under physiological conditions (Fig. S7).

Quantitative detection of ethanol by hPBNCs-AOx

Due to the high sensitivity of AOx toward alcohol and the excellent catalytic activity of hPBNCs-AOx for H_2O_2, the possibility of hPBNCs-AOx to be used for alcohol sensing is subsequently evaluated. As exhibited in Fig. 4a, as the concentration of ethanol increases, the absorbance at 652 nm which indicates the amount of the oxidized TMB is intensified. The absorbance intensity increases obviously with the low concentrations of ethanol but becomes gently when the concentration exceeds 500 μg·mL^{-1}. Critically, the plot displays a linear relationship in the low concentration region (c = 2–25 μg·mL^{-1}) (Fig. 4b). The limit of detection is calculated to be 1.41 μg·mL^{-1}, which is comparable to the previous

Table 1 The comparison of the analytical performance of this method for ethanol detection with previous colorimetric methods

Probe	LOD	Detection range	References
copper(II) complexes	0.8%	1–40%	[11]
SWCNT wrapped fiber	< 50 ppm	0–500 ppm	[12]
GO-coated and tapered fiber	1.330%	5–40% in water	[14]
MnO_2-ADH	5.0 μM	0.01–10 mM	[15]
HRP-AOx	2.1×10^{-3} g·L^{-1}	0.005–0.1 g·L^{-1}	[21]
Fe_3O_4-AOx	25 μM	100–500 μM	[22]
hPBNCs-AOx	1.41 μg·mL^{-1}	2–500 μg·mL^{-1}	This work

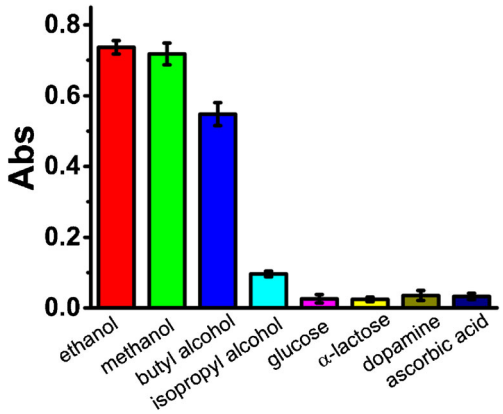

Fig. 5 Selectivity of the ethanol sensor. The absorption at 652 nm of the reaction solution after the introduction of different biomolecules. The final concentration of each compound was 5 mg·mL^{-1}. (Mean ± SD, n = 3 for each sample)

reported colorimetric methods for ethanol detection (Table 1). It is well known that alcohol concentration in blood especially in serum is a diagnostic and therapeutic target for alcoholism [2, 3, 33]. Based on this, it is of great importance to perform the experiment with serum samples to determine whether the hPBNCs-AOx can be used to monitor alcohol in biological matrix. As depicted in Fig. 4c and d, addition of serum containing different concentrations of ethanol into the mixture of TMB and hPBNCs-AOx induces different degree of oxidation of TMB, which is quite similar with the pure ethanol samples.

Selectivity

To evaluate the specificity of our system for alcohol detection, we next measured the effects of other biomolecules that are found abundantly in blood on the detection system. As displayed in Fig. 5, due to the high affinity of AOx toward shorter chain primary alcohols, only a distinct change of the absorbance intensity at 652 nm is found after the addition of primer aliphatic alcohols, especially for methanol and ethanol. While no noticeable absorbance change is observed from the initial solution containing glucose, α-lactose, dopamine or other non-alcohol biomolecule, which indicates that the assay exhibits a high selectivity for alcohol detection.

Determination of ethanol in blood

Inspired by the excellent performance of the synthesized hPBNCs-AOx in sensing ethanol in serum, we extend our work to real-time track the concentration of ethanol in blood serum after intragastric administration of mice with ethanol. Following a single 8 μL·g^{-1} injection of ethanol, the amount easily to induce alcohol intoxication [2, 3], the ethanol concentration rises quickly within 30 min, and reaches a peak at 60 min, which is calculated to 427 mg·dL^{-1} based on the standard curves. The ethanol concentration remains above 124 mg·dL^{-1} by 8 h after injection (Fig. 6a and Fig. S8a). Even reducing the amount of ethanol injected into the mice, the plasma ethanol concentrations are still high. Only the doses are lower than 1 μL·g^{-1} B.W., the plasma ethanol concentrations of animals are undetectable eight hours after injection (Fig. 6b and Fig. S8b). Critically, to verify the precision and the accuracy of our assay, gas chromatography [34] and HRP-AOx based assay [35] are also employed to carry out the same experiment. As shown in Fig. S9, S10, S11 and S12, the blood ethanol concentration presents by our assay is consistent with those obtained from the two different methods. All these results demonstrate the practicality of our method to be used for determining blood ethanol levels in real time, indicating its possibility to monitor alcohol consumption and study the ethanol toxicokinetics.

In the determination of ethanol, due to the ability of AOx to catalytic the primer aliphatic alcohols, our assay can only be used to monitor the concentrations of all alcohols in the samples, and the distinction between ethanol and other primer alcohols cannot be determined by the assay. Therefore, further effort is needed to explore other nanozyme-based assays for evaluation of different alcohols more comprehensively.

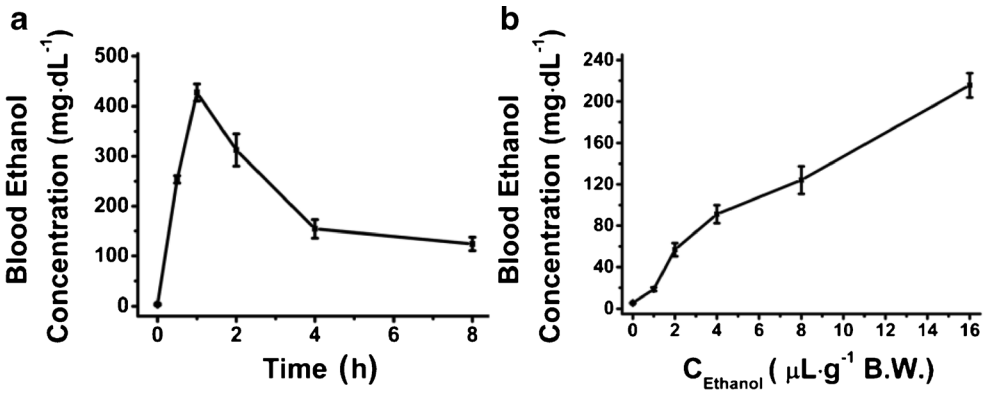

Fig. 5 Analysis of ethanol in real blood samples. **a** The blood ethanol concentration as a function of time after intragastric administration of mice with ethanol. The concentration of ethanol injected was 8 μL·g^{-1} B.W.. **b** The blood alcohol concentration as a function of ethanol concentration after injection of mice with different concentrations of ethanol for 8 h. (Mean ± SD, n = 6 for each group)

Conclusions

A colorimetric assay is described for sensitively and accurately monitoring ethanol utilizing the peroxidase-like activity of hPBNCs and the ethanol conversion enzyme, AOx. This colorimetric assay, with a low detection limit (1.41 $\mu g \cdot mL^{-1}$), was successfully used for the determination of the ethanol levels in blood, which was critically important for monitoring the alcohol consumption and studying the ethanol toxicokinetics. The method correlates well with data obtained by gas chromatography and HRP-AOx based assay. Crucially, when change AOx to other oxidase such as glucose oxidase, our system can also be used as glucose detector. The present method can be developed for high-throughput screening of alcohol consumption inhibitors and be of great use for designing multifunctional materials for a wide range of applications in biocatalysis, bioanalysis and nanobiomedicine.

Acknowledgements Financial support was provided by the National Natural Science Foundation of China (Grant No.21807024), the Youth Top-notch Talents Supporting Plan of Hebei Province (BJ2018007), the Hundred Persons Plan of Hebei Province (E2018050012), and the Natural Science Foundation of Hebei Province (Grant Nos. H2016206280 and H2017206281).

References

1. Voas RB, Fell JC (2010) Preventing alcohol-related problems through health policy research. Alcohol Res Health 33:18–28
2. Chen X, Cai F, Guo S, Ding F, He Y, Wu J, Liu C (2014) Protective effect of Flos puerariae extract following acute alcohol intoxication in mice. Alcohol Clin Exp Res 38:1839–1846
3. Liu Y, Du J, Yan M, Lau MY, Hu J, Han H, Yang OO, Liang S, Wei W, Wang H, Li J, Zhu X, Shi L, Chen W, Ji C, Lu Y (2013) Biomimetic enzyme nanocomplexes and their use as antidotes and preventive measures for alcohol intoxication. Nat Nanotechnol 8:187–192
4. Rocchitta G, Secchi O, Alvau MD, Migheli R, Calia G, Bazzu G, Farina D, Desole MS, O'Neill RD, Serra PA (2012) Development and characterization of an implantable biosensor for telemetric monitoring of ethanol in the brain of freely moving rats. Anal Chem 84:7072–7079
5. Kim J, Jeerapan I, Imani S, Cho TN, Bandodkar A, Cinti S, Mercier PP, Wang J (2016) Noninvasive alcohol monitoring using a wearable tattoo-based iontophoretic-biosensing system. ACS Sens 1:1011–1019
6. Selvam AP, Muthukumar S, Kamakoti V, Prasad S (2016) A wearable biochemical sensor for monitoring alcohol consumption lifestyle through ethyl glucuronide (EtG) detection in human sweat. Sci Rep 6:23111
7. Mohan AMV, Windmiller JR, Mishra RK, Wang J (2017) Continuous minimally-invasive alcohol monitoring using microneedle sensor arrays. Biosens Bioelectron 91:574–579
8. Wasfi IA, Al-Awadhi AH, Al-Hatali ZN, Al-Rayami FJ, Al Katheeri NA (2004) Rapid and sensitive static headspace gas chromatography-mass spectrometry method for the analysis of ethanol and abused inhalants in blood. J Chromatogr B Anal Technol Biomed Life Sci 799:331–336
9. Lidén H, Vijayakumar AR, Gorton L, Marko-Varga G (1998) Rapid alcohol determination in plasma and urine by column liquid chromatography with biosensor detection. J Pharm Biomed Anal 17:1111–1128
10. Sharma K, Sharma SP, Lahiri SC (2010) Estimation of blood alcohol concentration by horizontal attenuated total reflectance-Fourier transform infrared spectroscopy. Alcohol 44:351–357
11. El Bakkari M, Luguya R, Correa R, Vincent J (2008) A copper (II)-based multiphasic fluorous colorimetric ethanol assay. New J Chem 32:193–196
12. Manivannan S, Saranya AM, Renganathan B, Sastikumar D, Gobi G, Park KC (2012) Single-walled carbon nanotubes wrapped polymethyl methacrylate fiber optic sensor for ammonia, ethanol and methanol vapors at room temperature. Sensors Actuators B Chem 171–172:634–638
13. Girei SH, Shabaneh AA, Mohd HN, Hamidon MN, Mahdi MA, Yaacob MH (2015) Tapered optical fiber coated with graphene based nanomaterials for measurement of ethanol concentrations in water. Opt Rev 22:385–392
14. Zhu S, Lei C, Sun J, Zhao X-E, Wang X, Yan X, Liu W, Wang H (2019) Probing NAD^+/NADH-dependent biocatalytic transformations based on oxidase mimics of MnO_2. Sensors Actuators B Chem 282:896–903
15. Zhang Y, Li J, An G, He X (2010) Highly porous SnO_2 fibers by electrospinning and oxygen plasma etching and its ethanol-sensing properties. Sensors Actuators B Chem 144:43–48
16. Tian J, Deng S, Li D, Shan D, He W, Zhang X, Shi Y (2013) Bioinspired polydopamine as the scaffold for the active AuNPs anchoring and the chemical simultaneously reduced graphene oxide: characterization and the enhanced biosensing application. Biosens Bioelectron 49:466–471
17. Thungon PD, Kakoti A, Ngashangva L, Goswami P (2017) Advances in developing rapid, reliable and portable detection systems for alcohol. Biosens Bioelectron 97:83–99
18. Chinnadayyala SR, Santhosh M, Singh NK, Goswami P (2015) Alcohol oxidase protein mediated in-situ synthesized and stabilized gold nanoparticles for developing amperometric alcohol biosensor. Biosens Bioelectron 69:155–161
19. Das M, Goswami P (2013) Direct electrochemistry of alcohol oxidase using multiwalled carbon nanotube as electroactive matrix for biosensor application. Bioelectrochemistry 89:19–25
20. Alhadeff EM, Salgado AM, Cós O, Pereira N, Valero F, Valdman B (2008) Integrated biosensor systems for ethanol analysis. Appl Biochem Biotechnol 146:129–136
21. Il Kim M, Shim J, Parab HJ, Shin SC, Lee J, Park HG (2012) A convenient alcohol sensor using one-pot nanocomposite entrapping alcohol oxidase and magnetic nanoparticles as peroxidase mimetics. J Nanosci Nanotechnol 12:5914–5919
22. Fu X, Zhang H, Xiao J, Liu S (2012) Enzymatic detection of ethanol based on H_2O_2 sensitive quantum dots. J Cent South Univ 19: 3040–3045
23. Nasir M, Nawaz MH, Latif U, Yaqub M, Hayat A, Rahim A (2017) An overview on enzyme-mimicking nanomaterials for use in electrochemical and optical assays. Microchim Acta 184:323–342
24. Gao L, Zhuang J, Nie L, Zhang J, Zhang Y, Gu N, Wang T, Feng J, Yang D, Perrett S, Yan X (2007) Intrinsic peroxidase-like activity of ferromagnetic nanoparticles. Nat Nanotechnol 2:577–583
25. Song Y, Qu K, Zhao C, Ren J, Qu X (2010) Graphene oxide: intrinsic peroxidase catalytic activity and its application to glucose detection. Adv Mater 22:2206–2210
26. Cheng H, Liu Y, Hu Y, Ding Y, Lin S, Cao W, Wang Q, Wu J, Muhammad F, Zhao X, Zhao D, Li Z, Xing H, Wei H (2017) Monitoring of heparin activity in live rats using metal–organic framework nanosheets as peroxidase mimics. Anal Chem 89: 11552–11559

27. Niu X, Xu X, Li X, Pan J, Qiu F, Zhao H, Lan M (2018) Surface charge engineering of nanosized CuS via acidic amino acid modification enables high peroxidase-mimicking activity at neutral pH for one-pot detection of glucose. Chem Commun 54:13443–13446
28. Niu X, He Y, Zhang W, Li X, Qiu F, Pan J (2018) Elimination of background color interference by immobilizing Prussian blue on carbon cloth: a monolithic peroxidase mimic for on-demand photometric sensing. Sensors Actuators B Chem 256:151–159
29. Zhou D, Zeng K, Yang M (2019) Gold nanoparticle-loaded hollow Prussian blue nanoparticles with peroxidase-like activity for colorimetric determination of L-lactic acid. Mikrochim Acta 186:121
30. Wu T, Hou W, Ma Z, Liu M, Liu X, Zhang Y, Yao S (2019) Colorimetric determination of ascorbic acid and the activity of alkaline phosphatase based on the inhibition of the peroxidase-like activity of citric acid-capped Prussian blue nanocubes. Mikrochim Acta 186:123
31. Zhu W, Liu K, Sun X, Wang X, Li Y, Cheng L, Liu Z (2015) Mn^{2+}-doped prussian blue nanocubes for bimodal imaging and photothermal therapy with enhanced performance. ACS Appl Mater Interfaces 7:11575–11582
32. Chen Z, Chen C, Huang H, Luo F, Guo L, Zhang L, Lin Z, Chen G (2018) Target-induced horseradish peroxidase deactivation for multicolor colorimetric assay of hydrogen sulfide in rat brain microdialysis. Anal Chem 90:6222–6228
33. Savola O, Niemelä O, Hillbom M (2004) Blood alcohol is the best indicator of hazardous alcohol drinking in young adults and working-age patients with trauma. Alcohol Alcohol 39:340–345
34. Chen WJ, Parnell SE, West JR (2001) Nicotine decreases blood alcohol concentration in neonatal rats. Alcohol Clin Exp Res 25: 1072–1077
35. Gonchar MV, Maidan MM, Pavlishko HM, Sibirny AA (2001) A new oxidase-peroxidase kit for ethanol assays in alcoholic beverages. Food Technol Biotechnol 39:37–42